



Effect of Oil Type on Momentum, Heat, and Mass Transfer During Deep-Fat Frying of Potato Strips: Numerical and Experimental Study

Abdurrahman Ghaderi^{1,2} · Jalal Dehghannya¹ · Babak Ghanbarzadeh¹



Received: 30 April 2023 / Accepted: 5 July 2024

© The Author(s), under exclusive licence to European Association for Potato Research 2024

Abstract

The type of oil used during deep-fat frying can play a unique role in the transfer phenomena due to their different physicochemical properties. The effects of three types of oil, including canola, sunflower, and soybean oils, on the momentum, heat, and mass transfer during frying of potato strips were evaluated. The results showed that the oil type did not have a significant effect on moisture loss and oil uptake. However, the velocity distribution patterns of the three oils were not the same. The average simulated velocity for soybean oil was higher than those of the other two, attributable to its higher density. The results showed that the surface temperature of potatoes was affected by oil type. Overall, the developed numerical simulation could help in a better comprehension of the deep-fat frying of potato strips with the ultimate aim of producing low-fat quality products.

Keywords Frying · Heat transfer · Mass transfer · Modeling · Stefan's problem

Nomenclature

c	Concentration (mol m^{-3})
C_p	Specific heat capacity ($\text{J kg}^{-1} \text{K}^{-1}$)
D	Diffusion coefficient ($\text{m}^2 \text{s}^{-1}$)
D_{exp}	Experimental value
D_m	Mass diffusivity ($\text{m}^2 \text{s}$)
D_{sim}	Simulated value
$d.b$	Dry base (kg kg^{-1})
E_a	Activation energy (J mol^{-1})

✉ Jalal Dehghannya
J_dehghannya@tabrizu.ac.ir

¹ Department of Food Science and Technology, University of Tabriz, Tabriz 51666-16471, Iran

² Department of Food Science and Technology, University of Kurdistan, Sanandaj 66177-15175, Iran

g	Gravitational acceleration (m s^{-2})
h	Convective heat transfer coefficient ($\text{W m}^{-2} \text{K}^{-1}$)
h_m	Convective mass transfer coefficient (m s^{-1})
k	Thermal conductivity ($\text{W m}^{-1} \text{K}^{-1}$)
K_0	Evaporation rate constant (s^{-1})
K_w	Rate of evaporation (s^{-1})
L	Characteristic length (m)
M	Moisture content ($\text{kg}^{-1} \text{kg}$)
M_m	Molar mass (kg mol^{-1})
n	Unit normal vector to the boundary
n_d	Data points number
Nu	Nusselt number
P	Pressure (Pa)
$P\%$	Mean relative percent deviation
Pr	Prandtl number
R	Universal gas constant ($\text{J kmol}^{-1} \text{K}^{-1}$)
Ra	Rayleigh number
T	Temperature (K)
t	Time (s)
u	Velocity (m s^{-1})

Greek Symbols

α	Thermal diffusivity ($\text{m}^2 \text{s}^{-1}$)
β	Thermal expansion coefficient (K^{-1})
λ	Latent heat of evaporation (J kg^{-1})
μ	Dynamic viscosity (Pa s)
ν	Kinematic viscosity ($\text{m}^2 \text{s}^{-1}$)
ρ	Density (kg m^{-3})

Subscripts

a	Air
co	Core
cr	Crust
eq	Equilibrium
g	Gas
i	Initial
o	Oil
s	Solid
p	Potato
$surf$	Surface
v	Vapor
w	Water
∞	Surrounding air of fryer

Introduction

During deep-fat frying, the product is fried in various vegetable oils. The critical factors in choosing the type of oil include high stability at frying temperatures, high fluidity, reasonable prices, good taste, low tendency to form foam, smoke, or ageing, and increased oxidation stability of fried foods during storage (Brennan and Grandison 2012). The types of frying oil, owing to their various thermal and physicochemical properties, can affect momentum, heat, and mass transfer phenomena (Rahimi and Ngadi 2014; Troncoso and Pedreschi 2009). One of the factors affecting the heat transfer coefficient is the variation in the viscosity of the oil during the process due to polymerization reactions as well as the surface properties of the product (Dana and Saguy 2006). If the viscosity of the oil is lower, the heat transfer coefficient will increase (Mujumdar 2014). The low oil viscosity enhances the oil flow rate, leading to an increase in the heat transfer rate (Fellows 2017). In addition, the initial high viscosity or increased viscosity due to repeated use of oil (polymerization reactions) influences the momentum, heat, and mass transfer by influencing the movement of vapour bubbles during frying (Kalogianni et al. 2011).

By accurately predicting the distribution of the oil velocity and temperature, and the oil uptake and moisture loss, the frying process is better controlled with the ultimate goal of producing low-fat foods. Understanding the different oil uptake mechanisms during frying is essential to minimize oil uptake (Fellows 2017). Therefore, the study of the impact of other variables, including type of oil, on transport phenomena can help in better comprehension of the process. Frying oils are Newtonian fluids under normal frying conditions that have relatively high viscosity owing to their long chains. High-viscosity oils lead to increased oil uptake owing to low oil drainage. Therefore, the use of oils with lower viscosity can help minimize oil uptake (Ziaififar 2008). Additionally, oils with high viscosity can hinder the uniformity of frying, creating a heterogeneous distribution of velocity, temperature, and moisture during frying.

A review of the current literature on deep-fat frying indicates that there are no studies on the impact of the oil type on coupled momentum, heat, and mass transfer modeling (Southern et al. 2000; Naghavi et al. 2018; Ghaderi et al. 2018; Warning et al. 2012; Carrieri et al. 2010). Safari et al. (2018) reviewed methods and factors influencing heat and mass transfer coefficients during deep-fat frying. However, no momentum, heat, and mass transfer modeling was performed in this study. Dash et al. (2020) reviewed modeling procedures for heat transfer and case studies during deep-fat frying of food materials. Momentum and mass transfer modeling were not considered in this review. Gargari et al. (2022) performed heat and mass transfer modeling during deep-fat frying of a single potato, obtaining temperature distributions during the process. Momentum modeling to determine oil velocity distributions was not included in this study. Ghaderi et al. (2022) investigated the influence of potato to oil ratio on velocity, temperature, moisture, and oil distributions during frying using momentum, heat, and mass transfer modeling. However, the effect of oil type was not considered in their modeling.

Therefore, the present study aimed to develop a 3D model of the frying process to evaluate the effect of oil type, including sunflower, soybean, and canola oils, on the coupled transfer phenomena. This study may help improve the design of future fryer systems based on frying oil type.

Materials and Methods

Materials

Potatoes (cv. Agria) and sunflower, soybean, and canola oils as frying media were purchased. The potatoes were cut into $1.2 \times 1.2 \times 4$ cm³ pieces using a cutter. The frying was done in the frying loads of 1:15 (kg of the potato strips: the litre of the frying oil) at 170 °C for 1.5, 3, 4.5, and 6 min.

Measurement of Water and Oil Content

The water and oil contents of the potato strips were measured based on AOAC methods (AOAC 2012). The water content was obtained using oven drying at 105 °C until attaining a constant mass. Oil content was also measured by the Soxhlet method using petroleum ether.

Measurement of Temperature

The food and oil temperatures during frying were logged at 1-s intervals using twelve K-type thermocouples with a data logger. Nine thermocouples were used to record the center and surface temperatures of the four potato samples. In addition, the oil temperatures were recorded using three thermocouples placed at the top, middle, and base of the fryer, as shown in Fig. 1.

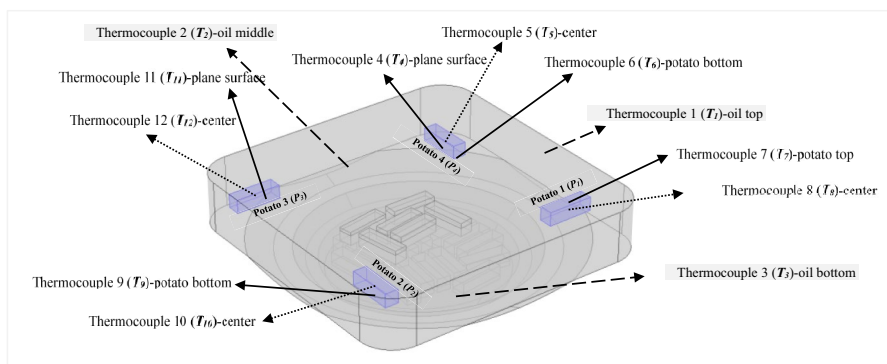


Fig. 1 Placement of thermocouples at 12 distinct positions of the potatoes and the frying oil

Model Development

Assumptions

- The thermophysical properties of the potatoes were considered uniform.
- The primary distribution of moisture and temperature in the potatoes was homogeneous.
- The frying oil was considered incompressible with variable properties.
- The formation of the crust and different properties of the crust and core were considered (Stefan or the moving boundary problem) (Farid 2002).
- Water evaporation was considered both on the surface and inside the food.

Governing Equations

A 3D unsteady-state numerical model was established to investigate the momentum, heat, and mass transfer in frying oils and potato strips.

Momentum Transfer in the Frying Oils The 3D velocity profile of the oils was obtained by the following equations (Carrieri et al. 2009):

$$\rho_o \left(\frac{\partial u}{\partial x} + \frac{\partial v}{\partial y} + \frac{\partial w}{\partial z} \right) = 0 \quad (1)$$

$$\rho_o \frac{\partial u}{\partial t} + \rho_o \left(u \frac{\partial u}{\partial x} + v \frac{\partial u}{\partial y} + w \frac{\partial u}{\partial z} \right) = \frac{\partial P}{\partial x} + \mu \left(\frac{\partial^2 u}{\partial x^2} + \frac{\partial^2 u}{\partial y^2} + \frac{\partial^2 u}{\partial z^2} \right) + \rho_o g_x \beta (T - T_0) \quad (2)$$

$$\rho_o \frac{\partial v}{\partial t} + \rho_o \left(u \frac{\partial v}{\partial x} + v \frac{\partial v}{\partial y} + w \frac{\partial v}{\partial z} \right) = \frac{\partial P}{\partial y} + \mu \left(\frac{\partial^2 v}{\partial x^2} + \frac{\partial^2 v}{\partial y^2} + \frac{\partial^2 v}{\partial z^2} \right) + \rho_o g_y \beta (T - T_0) \quad (3)$$

$$\rho_o \frac{\partial w}{\partial t} + \rho_o \left(u \frac{\partial w}{\partial x} + v \frac{\partial w}{\partial y} + w \frac{\partial w}{\partial z} \right) = \frac{\partial P}{\partial z} + \mu \left(\frac{\partial^2 w}{\partial x^2} + \frac{\partial^2 w}{\partial y^2} + \frac{\partial^2 w}{\partial z^2} \right) + \rho_o g_z \beta (T - T_0) \quad (4)$$

Slip boundary condition (B.C.) was applied at the oil and air interface:

$$n \cdot u = 0, t \cdot (-\nabla p + \mu_o \nabla^2 u) n = 0 \quad (5)$$

No slip B.C. was considered for the oil/potato boundaries and the fryer walls:

$$u = 0 \quad (6)$$

Heat Transfer in the Frying Oils The heat transfer in the oil phase was modeled using (Carrieri et al. 2009):

$$\rho_o C_{p,o} \frac{\partial T_o}{\partial t} + \rho_o C_{p,o} \left(\frac{\partial uT}{\partial x} + \frac{\partial vT}{\partial y} + \frac{\partial wT}{\partial z} \right) = \frac{\partial}{\partial x} \left(k_o \frac{\partial T_o}{\partial x} \right) + \frac{\partial}{\partial y} \left(k_o \frac{\partial T_o}{\partial y} \right) + \frac{\partial}{\partial z} \left(k_o \frac{\partial T_o}{\partial z} \right) \tag{7}$$

The heat flux B.C. (Eq. 8) for the oil/air interface, the temperature B.C. (Eq. 9) for the fryer element, and insulation B.C. (Eq. 10) were considered for the left walls of the fryer:

$$n \cdot k_o \nabla T_o = h_\infty (T_o - T_\infty) \tag{8}$$

$$T_o = T_{fryer} \tag{9}$$

$$n \cdot k_o \nabla T_o = 0 \tag{10}$$

The h_∞ was obtained by Eqs. 11, 12, and 13 (Purlis 2012):

$$Nu = \frac{h_\infty L}{k_a} = 0.54 Ra^{1/4} \tag{11}$$

$$Pr = \frac{\mu_a C_{p,a}}{k_a} \tag{12}$$

$$Ra = \frac{g \beta_a (T_o - T_\infty) L^3}{\nu_a^2} \times Pr \tag{13}$$

The temperature B.C. as a function of fryer temperature was considered due to the on/off automatic cycling of the element, as shown in Fig. 2a.

Mass Transfer (Vapour Distribution) in the Frying Oils The entrance of moisture in the form of vapour to the oil was modeled using (Carrieri et al. 2010, 2009):

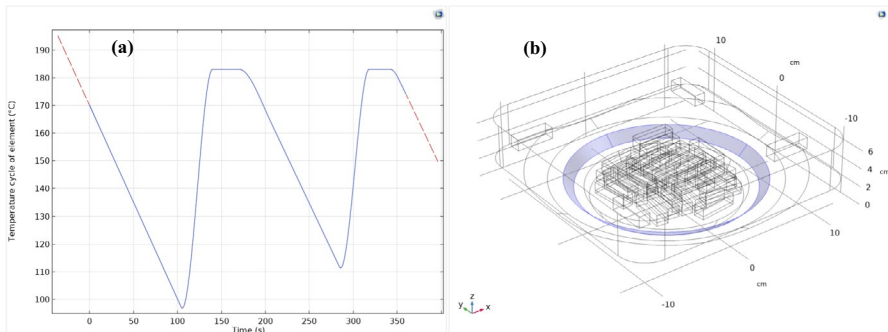


Fig. 2 Temperature cycling in the fryer element at ratio of 1:15 (a). Configuration of fryer element (blue colour) at the bottom of the fryer (b)

$$\frac{\partial c_{v,o}}{\partial t} = \frac{\partial}{\partial x} \left(D_{v,o} \frac{\partial c_{v,o}}{\partial x} \right) + \frac{\partial}{\partial y} \left(D_{v,o} \frac{\partial c_{v,o}}{\partial y} \right) + \frac{\partial}{\partial z} \left(D_{v,o} \frac{\partial c_{v,o}}{\partial z} \right) - \left(\frac{\partial uc_{v,o}}{\partial x} + \frac{\partial vc_{v,o}}{\partial y} + \frac{\partial wc_{v,o}}{\partial z} \right) \tag{14}$$

The boundary condition was considered mass flux (Eq. 15):

$$n.(D_{v,o} \nabla c_{v,o} + uc_{v,o}) = -h_{m,a}(c_{v,o} - c_{\infty}) \tag{15}$$

The $h_{m,a}$ was calculated using (Cengel 2006):

$$h_{m,a} = \frac{h_{\infty}}{\rho C_p} \tag{16}$$

Heat Transfer in the Potatoes The temperature distribution in the food was obtained using (Carrieri et al. 2010, 2009):

$$\rho_p C_{p,p} \frac{\partial T_p}{\partial t} = \frac{\partial}{\partial x} \left(k_p \frac{\partial T_p}{\partial x} \right) + \frac{\partial}{\partial y} \left(k_p \frac{\partial T_p}{\partial y} \right) + \frac{\partial}{\partial z} \left(k_p \frac{\partial T_p}{\partial z} \right) + K_w c_{w,p} M_w \lambda \tag{17}$$

where λ was expressed as (Bassama et al. 2012):

$$\lambda = 1000 \times (3174.95 - 2.46 \times T) \tag{18}$$

Also, the evaporation rate (K_w) was calculated using (Carrieri et al. 2009; De Bonis and Ruocco 2008):

$$K_w = \left(\frac{T_o}{T_{ref}} \right) K_0 \exp \left[\frac{E_a}{R} \left(\frac{1}{T_{ref}} - \frac{1}{T_p} \right) \right] \tag{19}$$

In Eq. 19, the K_0 was determined empirically (Feyissa et al. 2011, 2012; Ousegui et al. 2010). The E_a values calculated using Eq. 20 (Feyissa et al. 2011), and T_{ref} is the boiling point of the water.

$$E_a = \lambda \times M_w \tag{20}$$

where M_w is the water molecular weight.

The temperature continuity B.C. (Eq. 21) was imposed for all oil/potato interfaces (Dehghannya et al. 2011):

$$T_0 = T_p \tag{21}$$

Moreover, the moving B.C. (Stefan’s problem) was used with an interface temperature of 105 °C (Carrieri et al. 2009; Ghaderi et al. 2018).

Moisture (Liquid Water) Loss Distribution in the Potatoes The moisture removal from the potatoes in liquid form was modeled using (Carrieri et al. 2010):

$$\frac{\partial c_{w,p}}{\partial t} = \frac{\partial}{\partial x} \left(D_{w,p} \frac{\partial c_{w,p}}{\partial x} \right) + \frac{\partial}{\partial y} \left(D_{w,p} \frac{\partial c_{w,p}}{\partial y} \right) + \frac{\partial}{\partial z} \left(D_{w,p} \frac{\partial c_{w,p}}{\partial z} \right) - K_w c_{w,p} \tag{22}$$

The primary moisture content of potatoes was 82% (wet base). The no-flux B.C. was used, meaning that the removal of liquid water was not allowed from the product's surface (Ghaderi et al. 2018):

$$n.(D_{w,p} \nabla c_{w,p}) = 0 \tag{23}$$

Moisture (Water Vapour) Loss Distribution in the Potatoes The moisture removal from the potatoes in vapour form was modeled using (Carrieri et al. 2010):

$$\frac{\partial c_{v,p}}{\partial t} = \frac{\partial}{\partial x}(D_{v,p} \frac{\partial c_{v,p}}{\partial x}) + \frac{\partial}{\partial y}(D_{v,p} \frac{\partial c_{v,p}}{\partial y}) + \frac{\partial}{\partial z}(D_{v,p} \frac{\partial c_{v,p}}{\partial z}) + K_w c_{v,p} \tag{24}$$

The mass continuity boundary condition was considered:

$$c_{v,p} = c_{v,o} \tag{25}$$

Oil Uptake in the Potatoes Oil uptake into the potatoes was modeled using (Carrieri et al. 2010):

$$\frac{\partial c_o}{\partial t} = \frac{\partial}{\partial x}(D_o \frac{\partial c_o}{\partial x}) + \frac{\partial}{\partial y}(D_o \frac{\partial c_o}{\partial y}) + \frac{\partial}{\partial z}(D_o \frac{\partial c_o}{\partial z}) \tag{26}$$

The mass flux boundary condition was considered:

$$n.(D_o \nabla c_o) = h_{m,o}(C_{eq} - c_o) \tag{27}$$

The Chilton–Colburn analogy (Ventura et al. 2013), applying the findings of Yıldız et al. (2007), was used to calculate the $h_{m,o}$ as follows:

$$h_{m,o} = \frac{h_o}{\rho_o C_{p,o}} \left(\frac{D_{m,o}}{\alpha_o} \right)^{2/3} \tag{28}$$

where $D_{m,o}$ and α_o are the oil mass and thermal diffusivity obtained by Rojas et al. (2013).

Model Parameters

The model parameters and variables are presented in Table 1. When the temperature of the potatoes reached a boiling point (105 °C), the moisture evaporated, and a crust was created (Carrieri et al. 2009). Distinct thermophysical properties of the crust and core were considered in the modeling (Farid and Chen 1998) similar to Farkas et al. (1996). The properties used in Eqs. 11, 12, and 13 were obtained from the literature (Cengel 2006).

Numerical Solution

A 3D transient transport phenomena during frying was modeled using COM-SOL Multiphysics™ (version 5.4), based on finite elements. A mesh sensitivity

Table 1 Input parameters used in the simulations

Parameter	Symbol	Value/expression	Unit	Source
Density				
Potato crust	ρ_p	386	kg m ⁻³	Farid and Chen (1998)
Potato core	ρ_p	1132	kg m ⁻³	Farid and Chen (1998)
Sunflower oil	ρ_o	956.79–0.127T	kg m ⁻³	Rojas et al. (2013)
Soybean oil	ρ_o	1039.2–0.3975T	kg m ⁻³	Rojas et al. (2013)
Canola oil	ρ_o	990.07–0.2374T	kg m ⁻³	Rojas et al. (2013)
Specific heat capacity				
Potato crust	$C_{p,p}$	1790	J kg ⁻¹ K ⁻¹	Farid and Chen (1998)
Potato core	$C_{p,p}$	3450	J kg ⁻¹ K ⁻¹	Farid and Chen (1998)
Sunflower oil	$C_{p,o}$	3.1246T + 1262.7	J kg ⁻¹ K ⁻¹	Fasina and Colley (2008)
Soybean oil	$C_{p,o}$	2.9061T + 776.29	J kg ⁻¹ K ⁻¹	Fasina and Colley (2008)
Canola oil	$C_{p,o}$	3.0993T + 1242.7	J kg ⁻¹ K ⁻¹	Fasina and Colley (2008)
Thermal conductivity				
Potato crust	k	0.1	W m ⁻¹ K ⁻¹	Farid and Chen (1998)
Potato core	k	0.95	W m ⁻¹ K ⁻¹	Lioumbas et al. (2012)
Sunflower oil	k_o	4 × 10 ⁻⁰⁵ T + 0.1494	W m ⁻¹ K ⁻¹	Rojas et al. (2013)
Soybean oil	k_o	6 × 10 ⁻⁰⁵ T + 0.1348	W m ⁻¹ K ⁻¹	Rojas et al. (2013)
Canola oil	k_o	9 × 10 ⁻⁰⁵ T + 0.1394	W m ⁻¹ K ⁻¹	Rojas et al. (2013)
Viscosity				
Sunflower oil	μ_o	4.7738e ^{-0.016T}	Pa s	Fasina and Colley (2008)
Soybean oil	μ_o	4.4722e ^{-0.016T}	Pa s	Fasina and Colley (2008)
Canola oil	μ_o	3.3855e ^{-0.015T}	Pa s	Fasina and Colley (2008)
Thermal expansion coefficient				
Sunflower oil	β	8.07 × 10 ⁻⁴	K ⁻¹	Nita and Osman (2015)
Soybean oil	β	8.06 × 10 ⁻⁴	K ⁻¹	Nita and Osman (2015)
Canola oil	β	7.4 × 10 ⁻⁴	K ⁻¹	Nita and Osman (2015)
Diffusion coefficient				
Water in potato	D_w	2.2 × 10 ⁻⁸	m ² s ⁻¹	Granda (2006)
Vapour in potato and oil	D_v	2.6 × 10 ⁻⁶	m ² s ⁻¹	Thussu and Datta (2012)
Oil in potato	D_o	2.1 × 10 ⁻⁹	m ² s ⁻¹	Bansal et al. (2014)
Heat transfer coefficient	h_∞	Equation 11	W m ⁻² K ⁻¹	Cengel (2006)
Mass transfer coefficient	h_m	Equation 16	m s ⁻¹	Cengel (2006)
Rate of evaporation	K_w	Equation 19	s ⁻¹	Carrieri et al. (2010)
Gravitational acceleration	g	9.81	m s ⁻²	Cengel (2006)
Water molar mass	M_w	0.018	kg mol ⁻¹	Hädärugä et al. (2016)
Water evaporation latent heat	λ	Equation 18	J kg ⁻¹	Bassama et al. (2012)

examination was used to evaluate the influence of the mesh density on the predicted results. Therefore, various simulations with progressively finer meshes were considered until the mesh variation did not affect the results. A higher mesh density

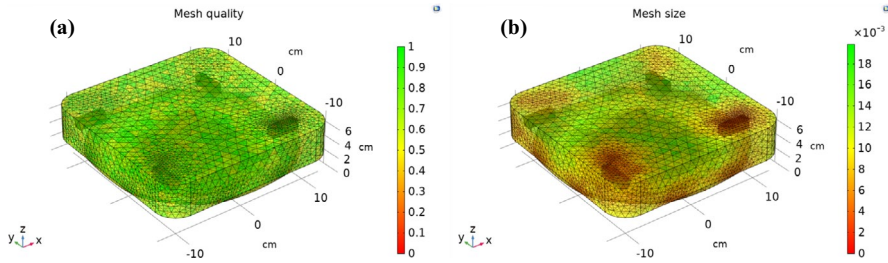


Fig. 3 Mesh quality (a) and mesh element size (cm) (b) used in the simulations

was selected in the proximity of the potato strips. The simulation domain was $25.5 \times 25.5 \times 7.5 \text{ cm}^3$. The mesh consisted of 273,482 elements (mostly tetrahedral), with a minimum element quality of 0.125. The mean mesh quality, volume ratio, and volume were 0.654, 4.01×10^{-4} , and 3860 cm^3 , respectively. The mesh quality and mesh element size are demonstrated in Fig. 3 for a frying load of 1/15. The experimental and predicted temperature data were monitored at 1-s intervals. The computation time for simulating the 6-min frying was 115 min by applying a computer system with two processors (Intel® Xeon® CPU, E5-2630 10-core, 2.20 GHz, 64 GB RAM).

Statistical Analysis

The R^2 and P% (mean relative error) were used to compare the experimental and simulated values. A mean relative error lower than 10% indicates goodness of fit (Polat et al. 2015). Analysis of variance was performed using SAS 9.4, and Duncan's test was used to investigate significant differences at the 5% probability level.

Results and Discussions

Oil Velocity Distribution

The oil velocity distributions for the various frying oils are shown in Fig. 4. The average velocities for the sunflower, soybean, and canola oils were 0.0018 , 0.0020 , and 0.0017 m s^{-1} , respectively. Although the type of oil did not have a significant effect on the average oil velocity, the velocity distributions were not identical (Fig. 4). The difference among the velocity distributions of various oils indicated that the oil type could somehow affect the velocity of the oil flow owing to differences in density, viscosity, and thermal expansion coefficient, each of which contributes to the momentum equation and leads to some variations in the oil velocity distributions. The mean velocity of soybean oil was higher than those of the other two oils. The thermal expansion coefficients of soybean and sunflower oils are approximately the same. Because the density of soybean oil is higher and its viscosity is lower, the average velocity for soybean oil was higher than those of the other oils.

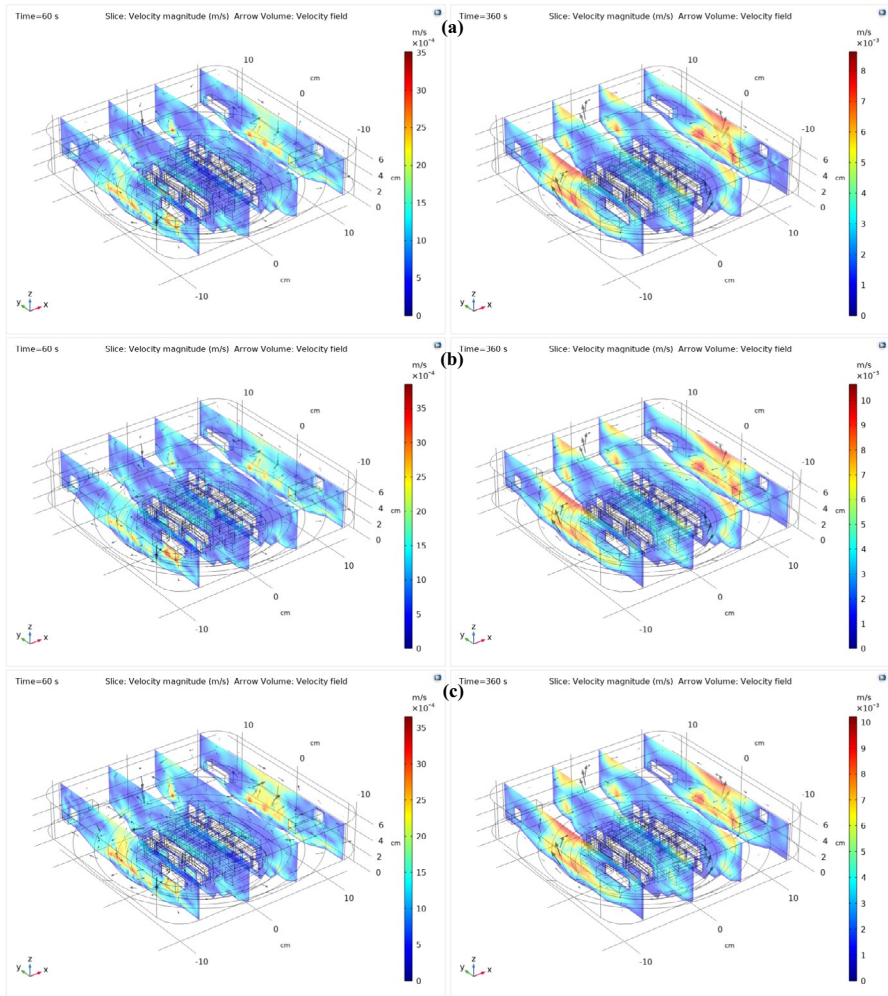


Fig. 4 Velocity distribution and arrow volume in 60 s (left) and 360 s (right) for canola (a), soybean (b), and sunflower (c) oils

Although canola oil has a higher density than the other two oils, its thermal expansion coefficient is lower, and its viscosity is higher, so its higher density cannot compensate for the high viscosity and low thermal expansion coefficient. Therefore, canola oil had the lowest average velocity.

Considering the velocity distributions (Fig. 4), there was a higher velocity in the areas of the heating element in all the frying oils owing to a higher buoyancy force when the temperature was applied through the component. The heterogeneity of the oil velocities was confirmed by the oil temperature distributions, as explained in detail in the “Temperature Distribution in Oil” section. The results showed that the oil velocity in the areas near the batch of potatoes was minimum,

whereas higher velocities were observed in the top parts of the fryer. The potatoes in the fryer base affected the flow behaviour of the oil and hindered its easy flow. Moreover, the high evaporation of moisture in these areas affects the buoyancy force of the oil. The oil velocity was indirectly validated using the experimental oil temperature data because of the impossibility of measuring the experimental velocities inside the batch fryer, as described by Deghannya et al. (2008).

Temperature Distribution in Oil

The temperature distribution profiles of sunflower, soybean, and canola frying oils are shown in Fig. 5. There was no considerable difference between the temperature

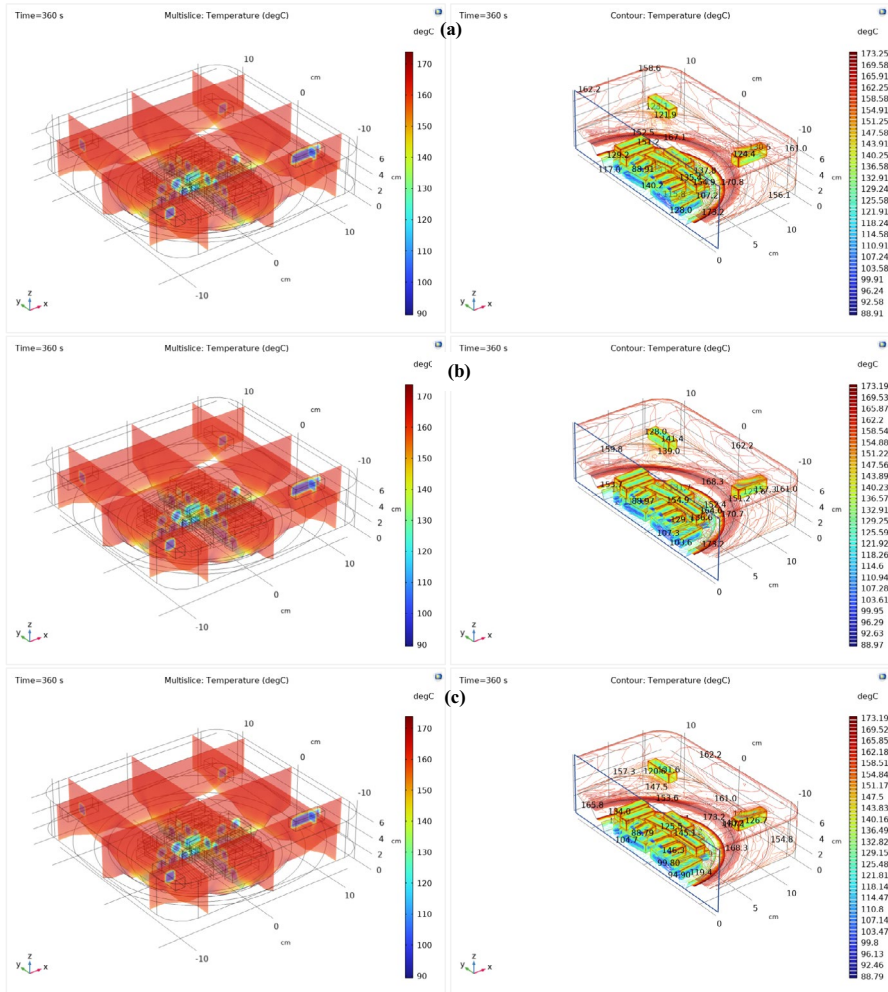


Fig. 5 Simulation of the oil temperature distribution in canola (a), soybean (b), and sunflower (c) after 360 s in multislice (right) and contour (left) views

distributions of the three oils with respect to their minimum and maximum temperatures. However, similar to the velocity distributions, non-uniform temperature distributions were also observed in the three frying oils. The temperature in all three oils was the lowest at the fryer's base, whereas the temperature near the heating element was the highest (Fig. 5). The reason for the high-temperature decline at the fryer's base was the high evaporation of water from the potato batch strips, which was not remunerated by the oil flow. Therefore, the temperature sharply decreased in these areas. A similar phenomenon was observed in the heating element, where the increase in temperature could not be immediately transferred by the oil flow to different fryer parts. Possible justifications for the nonuniformity of the oil temperature distributions throughout the fryer may be due to the effect of vapour bubbles on stirring oil and the laminar flow assumption for the frying process, in which only the buoyancy force leads to moving oil (Ghaderi et al. 2018).

According to Fig. 6a–c, for all frying oils, the highest difference between the predicted and experimental data was found at point 3 (T_3). This was due to the high evaporation of moisture as well as the predicted low velocity of the oils in this area (Fig. 4), where this temperature drop was not compensated by the heating element. When the potatoes came into contact with the oil, the oil temperature decreased (Fig. 6a–c). This decrease in oil temperature has also been reported in other studies (Lioumbas et al. 2012; Vitrac et al. 2003). The temperature drop was very intense in the first few seconds at fryer base (T_3), and the oil temperature decreased by approximately 15%, after which it was somewhat compensated by the oil flow.

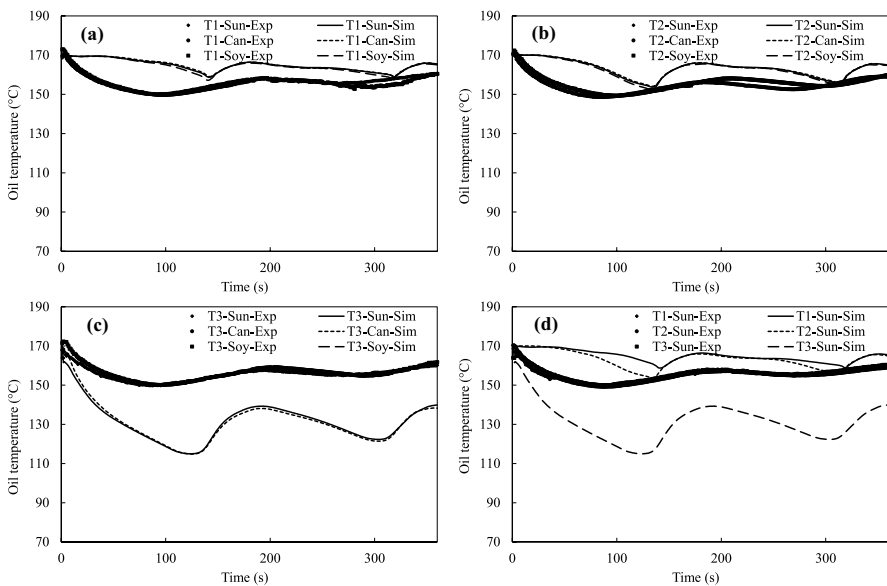


Fig. 6 Changes in experimental (Exp) and simulation (Sim) temperature of the frying oils at three different positions T1 (a), T2 (b), T3 (c), and comparison of the experimental and simulation data for sunflower (d)

The experimental oil temperatures at three different points in the fryer showed no considerable differences between the various oils. Lioumbas et al. (2012) reported the same temperature profile for two types of olive oil and palm oil under different frying conditions. They attributed the result to the similarity in the viscosities of the two oils and did not consider other parameters. In addition, the experimental data illustrated that the temperatures of the three distinct points of fryer (T_1 , T_2 , and T_3) was nearly identical, as shown in Fig. 6d, for example, for sunflower oil, mainly due to the agitation resulting from vapour bubbles. However, the simulated temperature data for the corresponding points were heterogeneous. The average temperature of the three points in the simulated and experimental data was approximately the same, with a standard deviation of ± 2 °C. The slight difference between these data indicates that the applied temperature of the heating element was reasonable.

Temperature Distribution in the Potatoes

The center temperature of the potato strips fried in the three types of oils demonstrated that the oil type did not significantly affect the temperature variation trend (Fig. 7). A minor decrease in the experimental center temperature of the potatoes occurred after 120 s which can be ascribed to crust formation when the transfer of heat to the potato center decreased. Because this occurs when the evaporation is at its maximum state, the decline in heat transfer leads to insufficient heat being transferred to the center to maintain a high temperature to keeping the former tendency. Therefore, the center temperature decreased. The temperature of the constant period for all treatments was approximately 96 °C, which was steady until the end of the process owing to the continuation of the evaporation process. Furthermore, the locations of the potatoes at four distinct fryer points did not show a substantial influence on the center temperature, as shown, for example, for two points (T_{10} and T_{12}). In general, Fig. 7 shows that the empirical center temperatures were predicted well with the simulation data for all three types of frying oils ($P < 3\%$, $R^2 = 0.98$). Only a slight difference was observed in the heating-up time when the rising rate of the empirical temperature increased. Similar findings have been reported by Lioumbas et al. (2012).

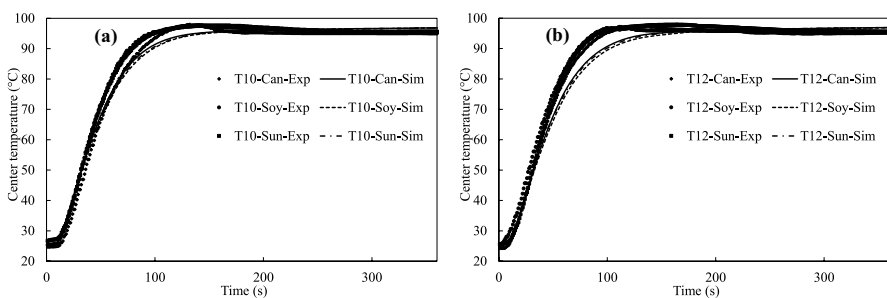


Fig. 7 Effect of the oil type on experimental (Exp) and simulation (Sim) temperature of the potato center at two locations of T10 (a) and T12 (b)

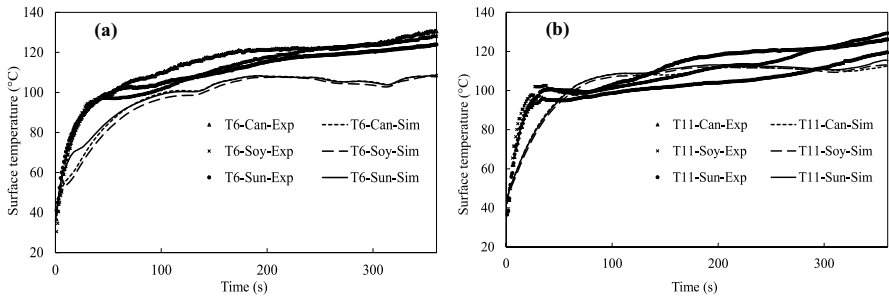


Fig. 8 Effect of the oil type on experimental (Exp) and simulation (Sim) surface temperature at two locations of T6 (a) and T11 (b)

In addition, the change in oil type led to variations in the surface temperatures (Fig. 8). Considering all frying oils, the upper surface of potato 1 (P_1) showed the lowest temperature (T_7), where a tiny oil layer (a few millimetres) streamed over the product. Regarding the low thickness of the oil and the cooling impact of the head-space air (Carrieri et al. 2010), the temperature at point T_7 was around the center temperature. In contrast, the results showed that a specific frying oil did not exhibit the highest surface temperature in any of the thermocouples. For example, sunflower oil showed the highest temperature in thermocouple 9 (T_9), whereas canola oil showed the highest temperature in thermocouple 6 (T_6). This result could be related to the proximity of the thermocouples to the heating element. A comparison of the experimental and simulated surface temperatures showed relatively good agreement ($P=8\%$, $R^2=0.75$). The relatively low R^2 could be due to the sensitive positions and placement of the thermocouples at a 1-mm distance under the surfaces of the potatoes. The thermocouple position and diameter can substantially influence the temperature measurement. Overall, the temperature differences between thermocouples at distinct surfaces of the potatoes can be attributed to the proximity of the potato to the heating element, orientation of the potato surface relative to the oil flow, effect of vapour bubbles in stirring the oil, creation of an insulation layer, and movement

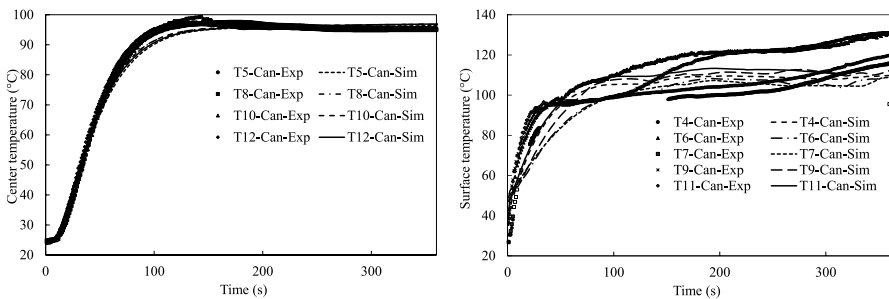


Fig. 9 Effect of the potatoes position on experimental (Exp) and simulation (Sim) temperature of the potatoes center (a) and surface (b)

of the thermocouple in this thin layer (Cebula 2016; Chen and Moreira 1997; Farid and Chen 1998; Farinu and Baik 2008).

The effect of the position of the potatoes on the temperature of the center and the surface in a specific frying oil, for example, canola (Fig. 9), confirmed the results illustrated in Figs. 7 and 8, indicating that the location had no sizable influence on the center temperatures, although the surface temperatures were significantly affected.

Furthermore, Fig. 10 shows that water evaporation began after approximately 40 s of frying. Until this time, no significant evaporation was observed owing to the lack of sufficient thermal flux to the center. In addition, almost 30% of the total water evaporated during approximately 90 s in the center, whereas 70% required approximately 270 s to evaporate. This decrease in evaporation rate (K_w) can be attributed to the reduction in water and thermal flux to the center due to the formation of a crust with low thermal conductivity. The reason for the relatively constant temperature of the center in all frying oils (Fig. 7) can also be interpreted according to the K_w (Fig. 10). As long as moisture is present in the center of the potatoes, the center temperature remains at the evaporation temperature, regardless of the type of oil, and after most of the water in the center has evaporated, the temperature of the center gradually rises towards the oil temperature.

The final temperature distributions of the central longitudinal cut potatoes after 360 s of frying with different frying oils showed that, generally, the center temperatures were not influenced by the oil type (Fig. 11). However, the surface temperatures were slightly affected by the oil type, especially the potato vertices. In addition, the temperature decreased from the edge to the center. Moreover, the temperature of all points of the potatoes, except 3 mm near the surface, was lower than 110 °C, indicating the remaining water in these areas. The temperature distributions in the potato strips were not symmetric, and the different sides showed various temperature distributions (Fig. 11). Axisymmetric heat diffusion has also been reported by Sahin et al. (1999) regarding the varied coefficients of heat transfer at the bottom and top of potatoes.

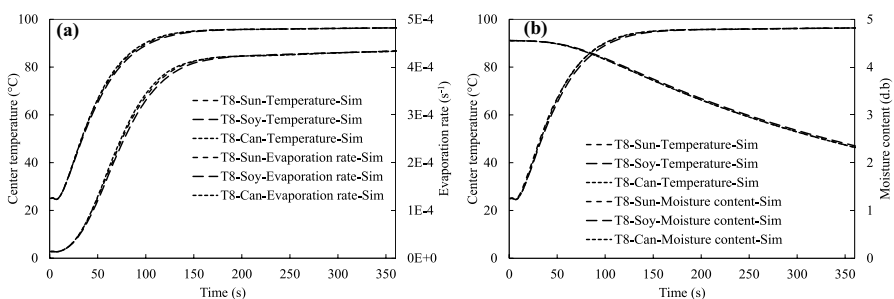


Fig. 10 Changes in the center temperature (Sim) of the potatoes vs. the evaporation rate over time for different oils (a) and changes in the center temperature (Sim) of the potatoes vs. moisture content over time for different oils (b)

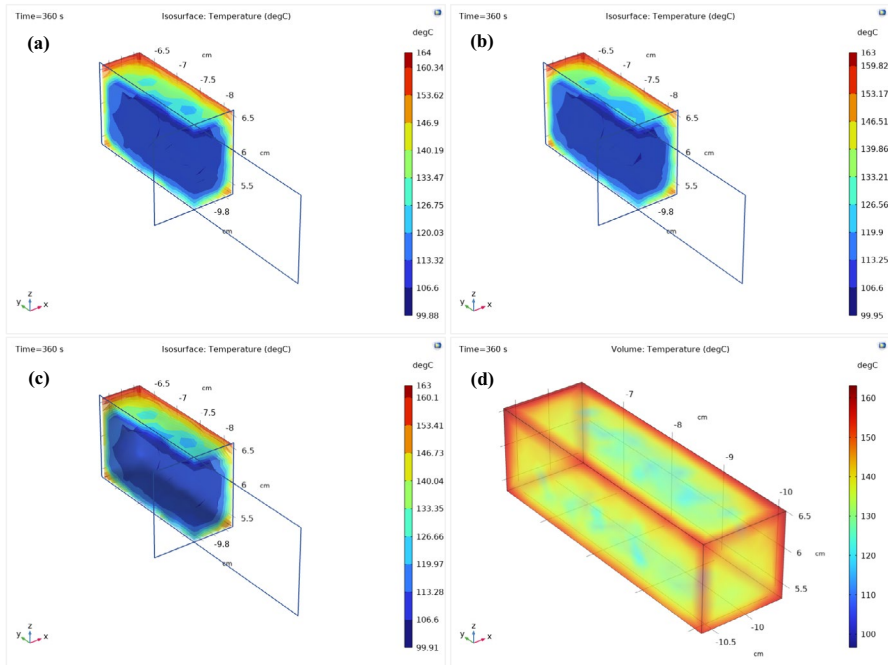


Fig. 11 Temperature isosurface view of the potatoes fried after 360 s in the canola (a), soybean (b), and sunflower (c) and volumetric view of the potato strip fried in soybean oil after 360 s

Moisture Removal and Oil Uptake in the Potatoes

The ultimate moisture and the oil uptake of the potatoes fried in three types of sunflower, soybean, and canola oils were 1.74, 1.75, 1.67 (d.b), and 0.17, 0.18, 0.2 (d.b), respectively. The type of oil had no substantial impact on the moisture removal and oil uptake. Similar results were obtained by Shallal et al. (2014) and Kim et al. (2010).

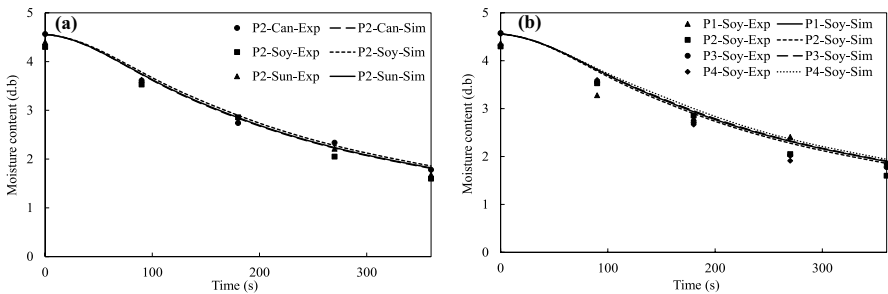


Fig. 12 Experimental (Exp) and simulation (Sim) moisture content of the potatoes fried in different oils (a) and in four fryer positions for soybean oil (b)

Moisture Removal in the Potatoes

The moisture content of the potatoes fried in sunflower, soybean, and canola oils were 1.82, 1.85, and 1.81 (d.b.), respectively (Fig. 12). Oil type did not considerably influence the moisture content of the potatoes. Similar findings were reported by Lioumbas et al. (2012), who showed that palm and olive oils had similar effects on the product moisture content. The empirical and simulated data showed good correlation ($R^2=0.98$ and $P=7.5\%$) (Fig. 12a). In addition, no considerable difference between the moisture contents of the samples was found for the four potato positions (Fig. 12 b). The slight overestimation of the simulation data could be because the potato strips were kept at ambient temperature for a few minutes to drain the surface oil before being placed in the oven to measure the moisture content. The cooling period reduced the moisture content of the samples. In addition, the absence of a substantial influence of the type of oil on the temperature of the potatoes (Figs. 7 and 8) indicates a lack of significant effect of the type of oil on the moisture content (Fig. 12). This is because moisture evaporation is affected by temperature and its result is reflected directly in the moisture content.

The moisture distribution in the central longitudinally cut potatoes for various frying oils is shown in Fig. 13. These findings reinforced that the type of oil did not influence the moisture content of the samples. In addition, the moisture content at the corners and vertices was minimal, matching the maximum temperatures in these

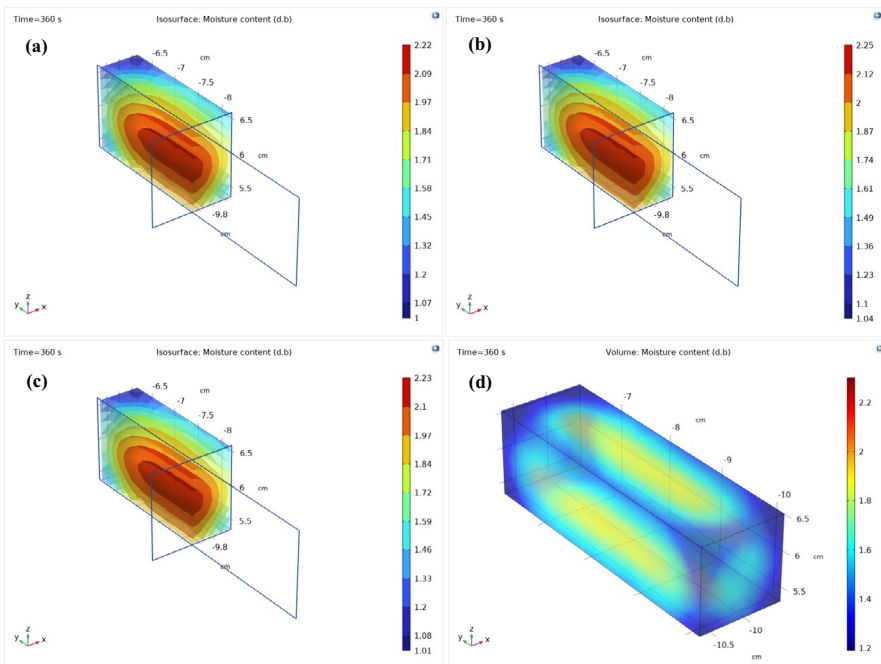


Fig. 13 Moisture isosurface view of the potatoes fried after 360 s in the canola (a), soybean (b), and sunflower (c) and volumetric view of the potato strip fried in sunflower oil (d)

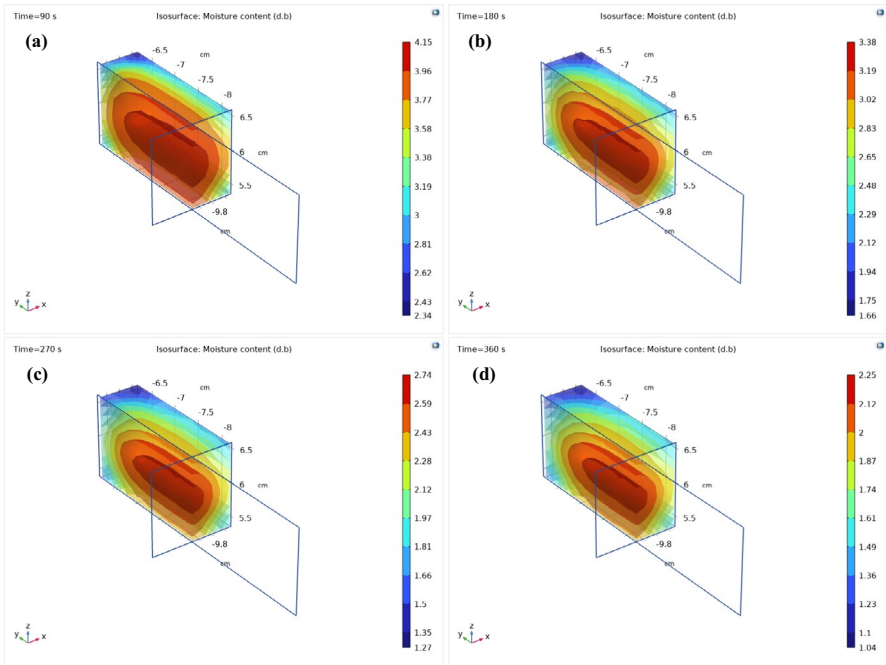


Fig. 14 Moisture isosurface view of the potatoes fried at 90 (a), 180 (b), 270 (c), and 360 s (d) in soybean oil

regions (Fig. 11). Approximately 65% of the moisture remained in the central part of the potato strips, where it prevented the temperature from increasing above the boiling point (Fig. 11). In addition, the changes in moisture distribution over time showed that the moisture content of the potatoes decreased, and the distribution of moisture at any given time was different (Fig. 14). Over time, the center moisture of the potatoes moved to the surface and then transferred to the oil. At the termination

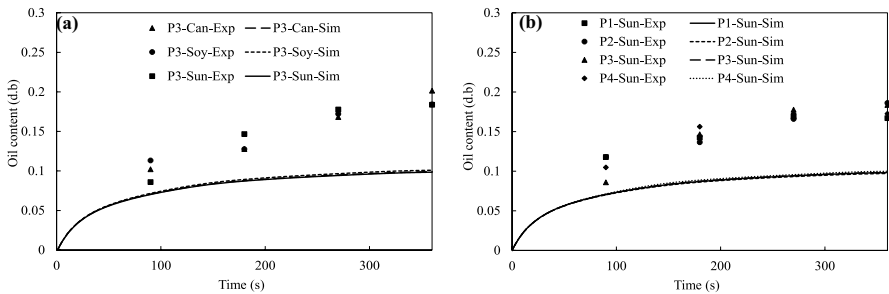


Fig. 15 Experimental (Exp) and simulation (Sim) oil content of the potatoes in three frying oils (a) and in four fryer positions in sunflower oil (b)

of frying, the moisture content of the edges was approximately 35%, illustrating that water remained in the potato center and even in the near-surface regions.

Oil Uptake in the Potatoes

Oil type did not have a considerable impact on oil absorption. Oil uptake increased over the frying time (Fig. 15), and the location of the potatoes did not have a substantial influence on the oil content (Fig. 15b). A weak agreement between the empirical and simulated data was observed ($P > 25\%$, $R^2 > 0.9$). An increase in the oil uptake during the cooling period caused by vapour condensation and partial suction of the surface oil could be a reason for the overestimation of the oil content (Dana and Saguy 2006).

Figure 16 shows the oil distribution of potatoes fried in the three types of oils with no considerable difference between the adsorbed oils. The maximum amount of absorbed oil was predicted on the outer surfaces of the potatoes, whereas the internal parts were almost oil-free. The edges and vertices of the potatoes showed more oil content owing to oil uptake from two or three directions (Fig. 16d). Figure 17 shows the oil uptake of fried potatoes in soybean oil. Oil uptake was limited to the crust areas, as oil absorption is a surface phenomenon (Tanguangdee et al. 2004). Bouchon et al. (2003) also reported similar results. In the simulations, the oil absorbed into the food at the end of frying was estimated to be 2 mm from the surface.

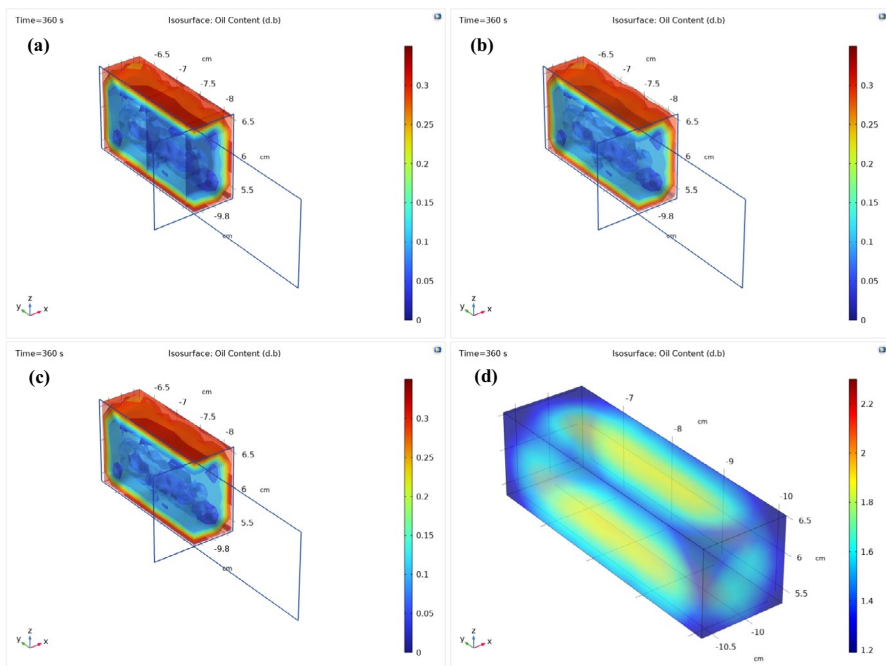


Fig. 16 Isosurface view of the oil uptake of the potatoes fried after 360 s in the canola (a), soybean (b), and sunflower (c) and volumetric view of potato fried in sunflower oil (d)

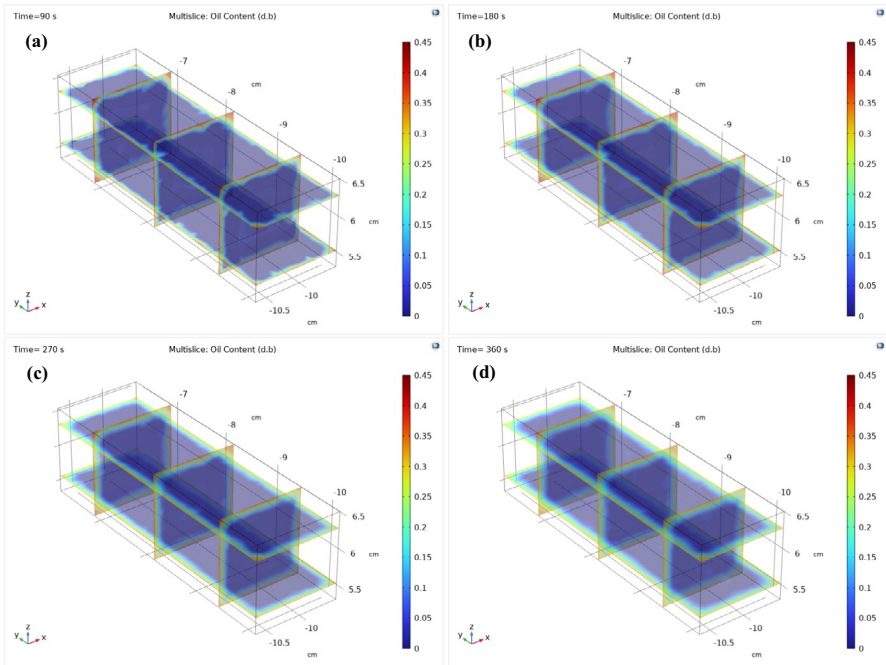


Fig. 17 Oil uptake in the potatoes fried in soybean oil at times 90 (a), 180 (b), 270 (c), and 360 s (d)

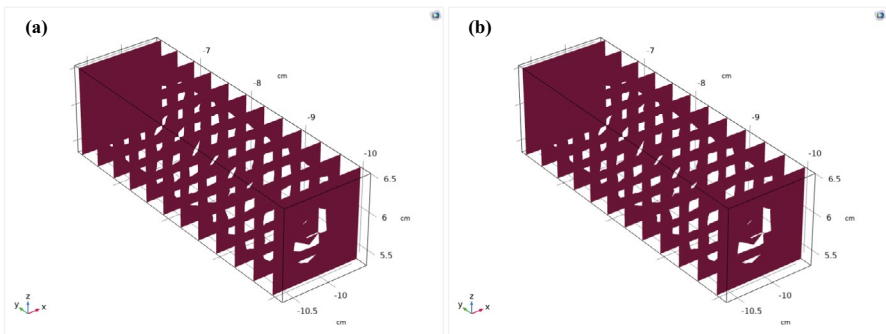


Fig. 18 Simulation of the crust formation in canola (a) and sunflower (b) oils after 360 s

According to Figs. 15 and 17, most of the oil uptake for all three types of oil occurred in the first 90 s of the frying process, and as the frying continued, very little oil was absorbed. This decrease in oil absorption can be ascribed to variations in the evaporation rate (Fig. 10) and crust formation (Fig. 18) in potatoes (Costa et al. 1999; Farid and Chen 1998). In Fig. 7, the center temperature of the potatoes reached a maximum after approximately 90 s. Additionally, the evaporation rate (Fig. 10) showed that the intensity of the evaporation rate in the central part of the potatoes increased after approximately 90 s. If vapour formation is maintained at a

suitable level, it could act as a sound barrier against oil diffusion into the inner parts of the potatoes. Besides, in terms of crust formation, most of the crust was formed on all sides of the potatoes during the first 90 s (data not shown). In other words, the gradual formation of the crust behaves as a barrier against oil uptake; therefore, the slope of oil uptake decreased over time (Fig. 15). In summary, the higher evaporation rate and crust formation synergistically decreased oil uptake after 90 s. Crust formation prevents oil uptake and diffusion into the central part. In addition, vapour production intensifies the effect of crust formation because the direction of the vapour flow is opposite to the diffusion of oil. These findings are in accordance with those of Pinthus et al. (1995) and Durán et al. (2007), who reported that oil absorption decreased with crust formation. However, there was no considerable difference between the thicknesses of the formed crust (Fig. 18) for the various frying oils. The same behaviour was observed for the evaporation rates (Fig. 10).

Sensitivity Analysis

The evaporation rate constant (K_0) is considered a practical and fundamental parameter in simulations of food processes to perform reasonable predictions comparable to experimental data (Ousegui et al. 2010). Therefore, a sensitivity analysis based on the effect of three different K_0 values of 5×10^{-3} , 5×10^{-4} , and $5 \times 10^{-5} \text{ s}^{-1}$ was performed on the surface and center temperatures, moisture content, and oil uptake of the potatoes. As shown in Fig. 19, the center and surface temperatures declined with an increase in the K_0 . This was because, when the evaporation rate increases, more

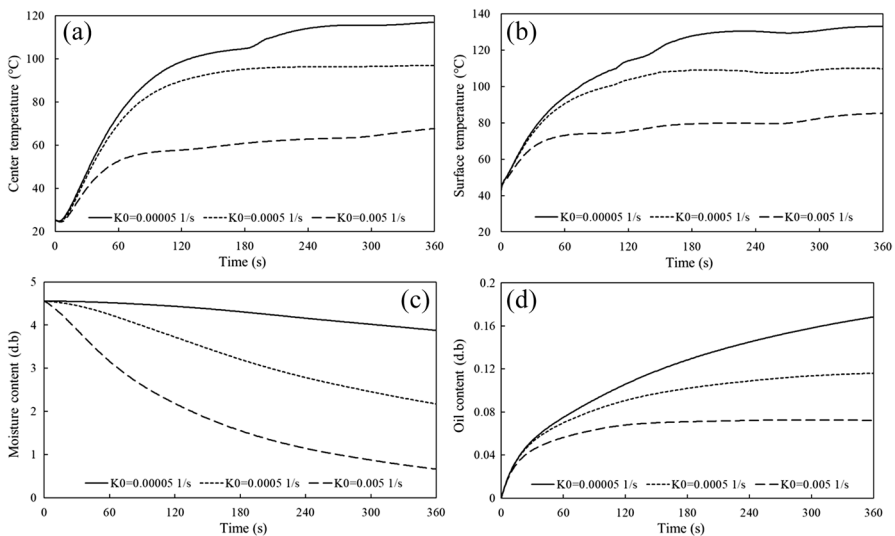


Fig. 19 Effect of the evaporation rate constant on center temperature (a), surface temperature (b), moisture content (c), and oil content (d) of the potatoes

water evaporates, and the energy needed for this evaporation prevents the temperature from rising beyond a specific limit.

However, with the decrease in the K_0 , because the evaporation rate decreases, the energy received by the potatoes is greater than the energy required for evaporation. Therefore, the center and surface temperatures are increased until, in this K_0 , an equilibrium is launched between the energy received and the water evaporated. This results in an equilibrium temperature that differs for different K_0 . In addition, the reason for the immediate temperature increase after approximately 180 s at the K_0 of $5 \times 10^{-5} \text{ s}^{-1}$ was the use of the moving boundary (Stefan) problem in the simulation when the temperature of a point in the potatoes exceeded 105 °C. This point was considered a crust, and since the crust had a lower heat capacity (1790 vs. 3450 J kg⁻¹ K⁻¹) and a lower density (386 vs. equal to 1132 kg m⁻³) relative to the core, a rapid rise in the center temperature was observed. In other words, a rise in temperature occurs when the heat flux remains constant and the heat capacity and density decrease.

Moreover, the moisture content and oil uptake of potatoes were considerably influenced by increasing or decreasing the K_0 . The reason for the drop in oil uptake with the increase in the K_0 is the drop in moisture content, and consequently, a rise in the percentage of dry matter. Because oil uptake is reported based on dry weight, the oil content will eventually decrease. The sensitivity analysis showed that all the variables used in the simulation, particularly, K_0 , significantly affected the simulation results. Therefore, proper values of the variables should be selected to achieve reliable outcomes.

Conclusion

The proper design of deep-fat frying contains various features of quality and operation that should be considered simultaneously. In this study, coupled modeling of the transfer phenomena was developed to investigate the effects of different frying oils (canola, sunflower, and soybean). Overall, although the applied frying oils each had different thermophysical properties, this difference was not significant enough to have a substantial impact on temperature, moisture removal, and oil absorption. In other words, if one attribute in oil was higher than that in the other oils, the same oil was lower in terms of another feature. Therefore, these differences in the various characteristics caused non-considerable differences in the results. Overall, although considering the moving boundary (Stefan) problem and the time-dependent temperature of the fryer's heating element considerably increased the accuracy of the simulation, the comparison of the experimental and simulation data showed that the vapour bubbles caused by moisture evaporation and the cooling phase after frying can significantly influence the reliability of the model. The results of this study could be useful for understanding process parameters, enhancing the quality of fried products, controlling the process, and designing frying apparatus.

Author contributions Abdurrahman Ghaderi: Methodology, software, formal analysis, investigation, resources, data curation, writing—original draft, visualization.

Jalal Dehghannya: Conceptualization, validation, writing—review and editing, supervision, project administration, funding acquisition.

Babak Ghanbarzadeh: Funding acquisition.

Data Availability All data generated or analyzed during this study are included in this manuscript.

Declarations

Ethics Approval Our research did not include studies on human subjects, human data or tissue, or animals.

Conflict of Interest The authors declare no competing interests.

References

- AOAC (2012) Official methods of analysis, 18th ed. Association of Official Analytical Chemists, Gaithersburg, USA
- Bansal HS, Takhar PS, Maneerote J (2014) Modeling multiscale transport mechanisms, phase changes and thermomechanics during frying. *Food Res Int* 62:709–717. <https://doi.org/10.1016/j.foodres.2014.04.016>
- Bassama J, Brat P, Boulanger R, Günata Z, Bohuon P (2012) Modeling deep-fat frying for control of acrylamide reaction in plantain. *J Food Eng* 113(1):156–166. <https://doi.org/10.1016/j.jfoodeng.2012.04.004>
- Bouchon P, Aguilera J, Pyle D (2003) Structure oil-absorption relationships during deep-fat frying. *J Food Sci* 68(9):2711–2716. <https://doi.org/10.1111/j.1365-2621.2003.tb05793.x>
- Brennan JG, Grandison AS (2012) Food processing handbook. John Wiley & Sons
- Carrieri G, Anese M, Quarta B, De Bonis MV, Ruocco G (2010) Evaluation of acrylamide formation in potatoes during deep-frying: the effect of operation and configuration. *J Food Eng* 98(2):141–149
- Carrieri G, De Bonis MV, Pacella C, Pucciarelli A, Ruocco G (2009) Modeling and validation of local acrylamide formation in a model food during frying. *J Food Eng* 95(1):90–98
- Cebula A (2016) A device for measuring the heat flux on the cylinder outer surface in a cross-flow. *Procedia Engineering* 157:264–270
- Cengel YA (2006) Heat and mass transfer: a practical approach. McGraw-Hill, New York
- Chen Y, Moreira R (1997) Modelling of a batch deep-fat frying process for tortilla chips. *Food Bioprocess* 75(3):181–190
- Costa RM, Oliveira FA, Delaney O, Gekas V (1999) Analysis of the heat transfer coefficient during potato frying. *J Food Eng* 39(3):293–299
- Dana D, Saguy IS (2006) Mechanism of oil uptake during deep-fat frying and the surfactant effect—theory and myth. *Adv Coll Interface Sci* 128:267–272
- Dash KK, Sharma M & Baren MA (2020) Modelling of heat transfer during deep fat frying of food. In: Sevdá S & Singh A (eds) *Mathematical and statistical applications in food engineering*. 1st edn. p[^]pp. CRC Press, Boca Raton. 398–421 <https://doi.org/10.1201/9780429436963-25>
- De Bonis MV, Ruocco G (2008) A generalized conjugate model for forced convection drying based on an evaporative kinetics. *J Food Eng* 89(2):232–240
- Dehghannya J, Ngadi M, Vigneault C (2008) Simultaneous aerodynamic and thermal analysis during cooling of stacked spheres inside ventilated packages. *Chem Eng Technol* 31(11):1651–1659
- Dehghannya J, Ngadi M, Vigneault C (2011) Mathematical modeling of airflow and heat transfer during forced convection cooling of produce considering various package vent areas. *Food Control* 22(8):1393–1399
- Durán M, Pedreschi F, Moyano P, Troncoso E (2007) Oil partition in pre-treated potato slices during frying and cooling. *J Food Eng* 81(1):257–265
- Farid M (2002) The moving boundary problems from melting and freezing to drying and frying of food. *Chem Eng Process* 41(1):1–10

- Farid M, Chen X (1998) The analysis of heat and mass transfer during frying of food using a moving boundary solution procedure. *Heat Mass Transf* 34(1):69–77
- Farinu A, Baik O-D (2008) Convective mass transfer coefficients in finite element simulations of deep fat frying of sweet potato. *J Food Eng* 89(2):187–194
- Farkas B, Singh R, Rumsey T (1996) Modeling heat and mass transfer in immersion frying I model development. *J Food Eng.* 29(2):211–226. [https://doi.org/10.1016/0260-8774\(95\)00072-0](https://doi.org/10.1016/0260-8774(95)00072-0)
- Fasina O, Colley Z (2008) Viscosity and specific heat of vegetable oils as a function of temperature: 35 C to 180 C. *Int J Food Prop* 11(4):738–746
- Fellows PJ (2017) *Food processing technology: principles and practice*. Woodhead Publishing, 4th edn. Cambridge, Cambridgeshire, United Kingdom. Elsevier
- Feyissa AH, Gernaey K, Ashokkumar S, Adler-Nissen J (2011) Modelling of coupled heat and mass transfer during a contact baking process. *J Food Eng* 106(3):228–235
- Feyissa AH, Gernaey KV, Adler-Nissen J (2012) Uncertainty and sensitivity analysis: mathematical model of coupled heat and mass transfer for a contact baking process. *J Food Eng* 109(2):281–290
- Gargari AN, Asefi N, Roufegarinejad L (2022) Simulation of heat transfer in deep fat frying of foods: an appropriate method for predicting the temperature distribution in a potato model. *Potato Res* 65(4):933–957
- Ghaderi A, Dehghannya J, Ghanbarzadeh B (2018) Momentum, heat and mass transfer enhancement during deep-fat frying process of potato strips: influence of convective oil temperature. *Int J Therm Sci* 134:485–499
- Ghaderi A, Dehghannya J, Ghanbarzadeh B (2022) Multiphase flow, heat and mass transfer modeling during frying of potato: effect of food sample to oil ratio. *Int J Food Eng* 18(5):337–358
- Granda CE (2006) Kinetics of acrylamide formation in potato chips. Texas A&M University. <https://doi.org/10.1016/j.foodchem.2021.129305>
- Hädärugă DI, Costescu CI, Corpaş L, Hädärugă NG, Isengard H-D (2016) Differentiation of rye and wheat flour as well as mixtures by using the kinetics of Karl Fischer water titration. *Food Chem* 195:49–55
- Kalogianni E, Karapantsios T, Miller R (2011) Effect of repeated frying on the viscosity, density and dynamic interfacial tension of palm and olive oil. *J Food Eng* 105(1):169–179
- Kim J, Kim DN, Lee SH, Yoo S-H, Lee S (2010) Correlation of fatty acid composition of vegetable oils with rheological behaviour and oil uptake. *Food Chem* 118(2):398–402
- Lioumbas JS, Kostoglou M, Karapantsios TD (2012) On the capacity of a crust–core model to describe potato deep-fat frying. *Food Res Int* 46(1):185–193
- Mujumdar AS (2014) *Handbook of industrial drying*. CRC Press
- Naghavi E-A, Dehghannya J, Ghanbarzadeh B (2018) 3D computational simulation for the prediction of coupled momentum, heat and mass transfer during deep-fat frying of potato strips coated with different concentrations of alginate. *J Food Eng* 235:64–78
- Nita I & Osman S (2015) Thermal expansion coefficient for different vegetable oils. In: *Food Chemistry & Engineering* 2015, Constanta, Romania., 15. <https://doi.org/10.1016/j.est.2023.106774>
- Ousegui A, Moresoli C, Dostie M, Marcos B (2010) Porous multiphase approach for baking process–explicit formulation of evaporation rate. *J Food Eng* 100(3):535–544
- Pinthus E, Weinberg P, Saguy I (1995) Oil uptake in deep fat frying as affected by porosity. *J Food Sci* 60(4):767–769
- Polat G, Baytekin S, Eray E (2015) Mark-up size estimation in railway projects using the integration of AHP and regression analysis techniques. *Procedia Engineering* 123:423–431
- Purlis E (2012) Baking process design based on modelling and simulation: towards optimization of bread baking. *Food Control* 27(1):45–52
- Rahimi J, Ngadi MO (2014) Inter-particle space fractions in fried batter coatings as influenced by batter formulation and pre-drying time. *LWT-Food Science and Technology* 57(2):486–493
- Rojas EEG, Coimbra JS, Telis-Romero J (2013) Thermophysical properties of cotton, canola, sunflower and soybean oils as a function of temperature. *Int J Food Prop* 16(7):1620–1629
- Safari A, Salamat R, Baik O-D (2018) A review on heat and mass transfer coefficients during deep-fat frying: determination methods and influencing factors. *J Food Eng* 230:114–123
- Sahin S, Sastry S, Bayindirli L (1999) Heat transfer during frying of potato slices. *LWT-Food Sci Technol* 32(1):19–24
- Shallal P, Rajaei P, Asadollahi S (2014) The effect of kind and temperature of oil used in deep frying on the amount of oil uptake. *Int J Biosci* 5(12):331–341

- Southern C, Farid M, Chen X, Howard B, Eyres L (2000) Thermal validation of a simple moving boundary model to determine the frying time of a thin potato crisp. *Heat Mass Transf* 36(5):407–412
- Tangduangdee C, Bhumiratana S, Tia S (2004) The role of moisture movement and crust thermal property on heat and mass process during deep-fat frying. *Int Commun Heat Mass Transfer* 31(1):73–84
- Thussu S, Datta AK (2012) Texture prediction during deep frying: a mechanistic approach. *J Food Eng* 108(1):111–121
- Troncoso E, Pedreschi F (2009) Modeling water loss and oil uptake during vacuum frying of pre-treated potato slices. *LWT-Food Sci Technol* 42(6):1164–1173
- Ventura M, Simionatto E, Andrade L, Simionatto E, Riva D, Lima S (2013) The use of thermal lens spectroscopy to assess oil–biodiesel blends. *Fuel* 103:506–511
- Vitrac O, Trystram G, Raoult-Wack A-L (2003) Continuous measurement of convective heat flux during deep-frying: validation and application to inverse modeling. *J Food Eng* 60(2):111–124
- Warning A, Dhall A, Mitrea D, Datta AK (2012) Porous media based model for deep-fat vacuum frying potato chips. *J Food Eng* 110(3):428–440
- Yıldız A, Palazoğlu TK, Erdoğdu F (2007) Determination of heat and mass transfer parameters during frying of potato slices. *J Food Eng* 79(1):11–17
- Ziaiiifar A-M (2008) Oil absorption during deep-fat frying: mechanisms and important factors. *AgroParisTech*

Publisher's Note Springer Nature remains neutral with regard to jurisdictional claims in published maps and institutional affiliations.

Springer Nature or its licensor (e.g. a society or other partner) holds exclusive rights to this article under a publishing agreement with the author(s) or other rightsholder(s); author self-archiving of the accepted manuscript version of this article is solely governed by the terms of such publishing agreement and applicable law.